Received: 10 April 2021 | Revised: 5 May 2021 | Accepted: 7 May 2021

DOI: 10.1002/pat.5397

RESEARCH ARTICLE

polymers for advanced technologies WILEY

Bilayer films of poly(ε-caprolactone) electrosprayed with gum rosin microspheres: Processing and characterization

Cristina Pavon[1] | Miguel Aldas[1,2] | Harrison De La Rosa-Ramírez[1] | María Dolores Samper[1] | Marina Patricia Arrieta[3,4] | Juan López-Martínez[1]

[1]Instituto de Tecnología de Materiales (ITM), Universitat Politècnica de València (UPV), Alcoy, Spain

[2]Departamento de Ciencia de Alimentos y Biotecnología, Facultad de Ingeniería Química y Agroindustria, Escuela Politécnica Nacional, Quito, Ecuador

[3]Departamento de Ingeniería Química Industrial y del Medio Ambiente, Escuela Técnica Superior de Ingenieros Industriales, Universidad Politécnica de Madrid (ETSII-UPM), Madrid, Spain

[4]Grupo de Investigación: Polímeros, Caracterización y Aplicaciones (POLCA), Madrid, Spain

Correspondence
Cristina Pavon, Laboratorio F3L5, Instituto Tecnológico de Materiales (ITM), Universitat Politècnica de València, Campus Alcoy, Plaza Ferrándiz y Carbonell N°1, Alcoy, Alicante 03801, Spain.
Email: crisppavonv@gmail.com

Funding information
Spanish Ministry of Economy and Competitiveness (MINECO), Grant/Award Number: PROMADEPCOL (MAT2017-84909-C2-2-R)

Bilayer systems, consisting of electrosprayed gum rosin microspheres (eGR) and poly (ε-caprolactone) (PCL), were prepared. First, the electrospraying processing conditions of GR in two different solvents, dichloromethane, and chloroform, were optimized. Various electrospraying polymeric solution flow rates and applied voltages were tested and morphologically analyzed in terms of particle size distribution and microspheres density. The conditions at which a homogeneous and narrow microspheres size distribution was achieved were chosen as the best for each solvent. The eGR was deposited onto a compression-molded PCL film to obtain the bilayer systems. The bilayer systems were characterized by their visual appearance, microstructural analyses, thermal and mechanical performance, and surface wettability. It was determined that the mechanical and thermal behavior of PCL film was not affected due to the addition of the eGR microspheres layer. Meanwhile, the eGR layer considerably changes the surface color of the PCL film, reduces the film transparency, and produces a blocking effect in the UVB region and high blockage in the UVA region. In addition, the microspheres layer presents a tunable hydrophobicity depending on the solvent used, reaching values of ultrahydrophobic surfaces. Thus, the obtained result reveals a great potential to easily process bilayer systems with high interest in sustainable agricultural, packaging, and/or biomedical applications.

KEYWORDS
bilayer, electrospraying, gum rosin, microspheres, poly(ε-caprolactone)

1 | INTRODUCTION

Polymer-based microspheres have gained importance in a broad range of fields during the last decade since they can be widely used in several industrial sectors such as chromatography separation, biomedical devices, coating additives, and controlled release reservoirs.[1–3] Polymer-based microspheres present a spherical geometrical shape and can be manufactured to have a uniform size that ranges from nanometer to micrometer scale.[1,2] These microspheres can be designed with functional properties such as uniform size and shape, larger surface area, and porous surface or hollow interior to allow the encapsulation of components.[4]

The preparation of polymer-based microspheres is usually developed by the techniques of solvent separation, single and double emulsion, spray-drying, freeze-drying, and coacervation technique.[5] However, most of the stated methods have disadvantages, such as some limitations to scale up, a big polydispersity in the particle size, and a restricted capacity to produce small particles.[4] Nonetheless, the electrospraying technique allows obtaining the microspheres, while

overcoming the problems associated with conventional particle-producing methods.[6]

Electrospraying is an electrohydrodynamic process, which allows the production of microspheres, with a narrow size distribution, by using a high-power electric field.[6–8] In the production process many parameters had to be handled for instance: the flow of the polymeric solution, the voltage applied to the capillary needle, and working distance (from the needle to the collector). In addition, the solution parameters such as composition, concentration, viscosity, conductivity, and surface tension, also affect the electrospraying.[7] Therefore, optimize an electrospraying process can be complex given the number of parameters that have to be handled.[8] Despite the drawbacks of the process, during the last years, several companies have commissioned plants for manufacturing electrospun materials. Thus, electrohydrodynamic processing has gained interest in the industrial sector due to its cost-effectiveness, high versatility, and opportunity to produce electrospun materials at the industrial level.[9]

Electrospraying has been investigated for uses in the field of pharmacy, cosmetics, ceramics, and the food industry.[10] Electrosprayed and electrospun polymers were studied as carriers for active compounds, due to the small diameters and large surfaces area with high porosity that is easy for functionalization.[9] It is possible to remark the study of Khan et al., which covers the effect of the different process and product parameters to obtain food coatings.[11] As well, Bock et al., analyzed the variation of different parameters in the electrospraying process to produce microspheres from solutions of different concentrations of poly(ε-caprolactone) in chloroform. Furthermore, these microspheres were proven to be compatible with cells, making them useful for biomedical applications.[8]

Gum rosin is the solid residue of pine resin, produced as a common defensive response of conifers to external factors.[12] Gum rosin is a thermoplastic, acidic, semi-transparent material with a yellowish coloration, and soluble in organic solvents.[13] Gum rosin is currently used in different applications such as in the paper industry, adhesives, plastics, printing inks, coatings, and in the food industry.[14–16] As a plastic additive, gum rosin has shown several interesting properties such as its ability to act as a light-absorbing agent, diminishing and/or preventing the transmission of light through plastics films.[17] Furthermore, gum rosin is generally studied, together with its derivatives, in the pharmaceutical industry, for coatings, microencapsulation, and controlled release of substances.[13,18] Poly(ε-caprolactone) (PCL) has been proven to work well with gum rosin, as both materials are biocompatible, biodegradable, and have similar melting points (around 60°C).[19] PCL is a semicrystalline biocompatible and biodegradable polymer with superior viscoelastic performance with interest in several industrial applications such as food packaging or biomedical devices.[20]

Regarding the use of gum rosin in electrohydrodynamic processes, Baek et al. established the appropriate concentration for the production of nanofibers from gum rosin solutions in chloroform and dichloromethane.[21] Nirmala et al. prepared PCL-based nanofibers with gum rosin in different concentrations. Its bactericidal effect provides the material with antimicrobial activity, with interest for uses in biomedical applications.[22] Whereas Nirmala et al. performed a comparison between gum rosin nanofibers obtained by electrospinning and thin gum rosin films as coatings, they found structural advantages in the use of nanofiber coatings such as large surface area, cylindrical morphology, and high porosity.[23] To the best of our knowledge, the production of gum rosin microspheres by the electrospraying technique has not been reported yet.

In this context, electrohydrodynamic process (electrospinning and electrospraying) are progressively becoming more widely recognized as a powerful tool for the development of bilayer films, having the main advantage to operate at room temperatures[9,24] at the same time as it represent an easy way for providing specific active functions (e.g., antioxidant, antimicrobial, etc.) by incorporating different active components.[25] Bilayer films are combinations of two different layers typically based on materials with dissimilar advantage properties glued together to fulfill an overall performance that monolayers do not offer.[24,26] Thus, bilayer systems based on biopolymers are specifically designed to improve some specific properties of biopolymers as they generally present poor water resistance and reduced mechanical performance.[9,24]

Thus, this work is aimed at developing scalable bilayer films based on an external layer of PCL film produced by a melt-blending approach and with an inner layer of gum rosin microspheres produced by the electrospraying technique. Gum rosin was selected as the inner layer with the main objective to provide hydrophobicity to the PCL layer. With this purpose, the electrospraying processing conditions of GR were optimized using two different solvents, chloroform (CF) and dichloromethane (DCM). These two solvents were selected due to their expected high evaporation rate (CF has a boiling point of 60°C and DCM has a boiling point of 40°C). The influence of the variation of the potential applied as well as the flow rate of the gum rosin solution in the production of electrospray gum rosin microspheres was studied and the best conditions were established to further produce electrospray GR microspheres with both studied solvents. Then, the microspheres were directly electrosprayed over a PCL film, and the bilayer systems were characterized through the evaluation of their microstructural, mechanical, and thermal performance. Some functional properties such as color properties, visible, and UV light transmission as well as surface wettability were also measured to get information about their potential use at the industrial level as functional materials providing UV blocking effect and water repellence.

2 | MATERIALS AND METHODS

2.1 | Materials

Gum rosin (GR) commercial-grade was supplied by Sigma-Aldrich (Mostoles, Spain) CAS Number: 8050-09-7, and it was used for the inner layer. GR is characterized by a molecular weight of 302 g/mol, a softening point of 66.5°C, an acid number of 167. Chloroform was supplied by Panreac (Barcelona, Spain) with a density >1.48 g/cm^3 at 20°C and 99.8% purity. Dichloromethane, provided by Sigma-Aldrich

(Madrid, Spain), had a density of 1.325 g/cm^3 at 20°C and 99.8% purity. Both products were used as solvents for the GR electrospraying forming solution. Polycaprolactone CapaTM 6800, commercial-grade, was used for the outer layer and was kindly supplied by Perstorp UK Ltd. (Warrington, UK). It has a density of 1.15 g/cm^3 and a melt flow index (MFI) of 2–4 g/10 min (160°C, 2.16 kg).

2.2 | Methods

2.2.1 | GR electrospraying optimization

The effect of the flow rate and the voltage applied over the production of GR microspheres, their size, and morphology was analyzed for all the processing conditions assayed. Two GR solutions were prepared: one of GR 60 w/v in dichloromethane (GR_{DCM}) and the other one of GR 45 w/v in chloroform (GR_{CF}). The solutions were kept under constant stirring at room temperature for 24 h. Electrospraying was done using a Higher Pressure Programmable Single Syringe Pump NE-1010 (Shropshire, UK), and a high voltage 0–30 kV power supply Genvolt 7xx30 series (Shropshire, UK). Each solution was fed into a 10-mL plastic syringe set in the pump. The syringe was connected through polytetrafluoroethylene (PTFE) tubes to a stainless-steel needle (Ø = 4.9 mm) while the needle tip was connected to the power supply. The working distance from the needle to the collecting plate was 15 cm. The microspheres were electrosprayed for 40 min and collected in a sheet of aluminum foil, which was placed over the rectangular metallic collecting plate. The process was carried out at 25°C and 40% RH.

The morphology of the obtained microspheres was analyzed by field emission scanning electron microscopy (FESEM), using a Zeiss Ultra 55 microscope at 1 kV. The density of microspheres and the size distribution characterization were calculated using the software ImageJ in the micrographs of the experiments in which electrospraying has produce GR microspheres. The significant differences were assessed at a 95% confidence level according to Tukey's test using a one-way analysis of variance (ANOVA). The conditions in which the obtained microspheres have had a narrow size distribution were selected for the preparation of PCL-eGR bilayers systems.

2.2.2 | Bilayer system preparation

The inner layer was prepared by electrospraying technique following the optimized conditions determined for electrospraying solution of GR in both DCM and CF. Gum rosin solutions were prepared and then electrosprayed over the PCL films for 4 h. The outer PCL layer was processed into films by compression molding at 80°C in a 10-Tn hydraulic press from Robima S.A. (Valencia, Spain) equipped with two hot aluminum plates and a temperature controller from Dupra S.A. (Castalla, Spain) by using a film mold (120 × 120 mm^2). PCL pellets were kept between the plates at atmospheric pressure for 1 min until melting and they were further submitted to a pressure of 50 MPa for 1 min and then quenched to room temperature for an additional 4 min.

Each GR electrospray forming solution was processed by electrospray process. For GR electrospraying solution prepared with DCM a flow rate of 1 μL/min was used and with an applied voltage of 10 kV (positive and negative voltages = 5 kV and −5 kV, respectively; Bilayer film label as PCL-eGR_{DCM}). For GR solution prepared with CF a flow rate of 5 μL/min was used and potential of 10 kV (positive and negative voltages = 5 kV and −5 kV; Bilayer film label = ePCL-cGR). Under these optimized processing conditions, the GR electrospray microspheres were poured onto the PCL films to obtain the bilayer systems. The PCL-eGR bilayer films were dried under vacuum at room temperature in a desiccator for 120 h to remove any residual solvents.

2.2.3 | Bilayer film characterization

Visual appearance, UV–Vis spectroscopic, and colorimetric analysis

Visual appearance was evaluated by visual inspection of neat PCL, neat GR, and the produced bilayers, and a comparison of the bilayer systems was done. UV–Vis spectroscopic analyses were carried out on a spectrophotometer Cary 100 UV–Vis by Agilent technologies (Barcelona, Spain), at a range between 200 and 800 nm to notice the optical changes due to the electrosprayed layer over the PCL film. The UV–Vis absorption spectra of PCL and that of PCL-eGR based bilayer films were obtained.

The surface color properties of the bilayer films were assessed on a Colorflex-Diff2 458/08 colorimeter from HunterLab (Reston, VA). For means of comparison, PCL monolayer film was used as a reference. The test was performed under the CIE L*a*b* color space, where L* stands for lightness, a* for green (−a*) to red (+a*) colorations, and b* from blue (−b*) to yellow (+b*) coloration.[27] The mean value and the standard deviation of L*, a*, and b* coordinates, and the yellowness index (YI) is reported. Moreover, the total color differences (ΔE) were obtained comparing the microspheres side of the bilayer film with the PCL surface color using Equation (1).[27]

$$\Delta E = \sqrt{\Delta a^{*2} + \Delta b^{*2} + \Delta L^2} \quad (1)$$

The statistical differences in these properties were evaluated by the one-way ANOVA, at 95% confidence level according to Tukey's test.

Water contact angle measurement

Wettability was determined via the sessile drop method, with an optical goniometer EasyDrop-FM140 from Kruss Equipments (Hamburg, Germany). The water contact angle (WCA) of deionized water over the specimens' surface was measured and the mean value and standard deviation of 10 points are reported. The obtained results were statistically analyzed in the conditions previously reported.

Field emission scanning electron microscopy

Field emission scanning electron microscopy was conducted on a Zeiss Ultra 55 microscope at 1 kV. Before the analysis, PCL monolayer film as well as the ePCL-GR bilayer films were cryofractured after immersion in liquid nitrogen and then sputtered with a gold–palladium alloy in a Sputter Mod Coater Emitech SC7620, Quorum Technologies (East Sussex, UK).

Thermal analyses

Differential scanning calorimetry (DSC) experiments were conducted in a calorimeter Mettler DSC821e (Toledo, Spain) under a nitrogen atmosphere (flow rate 30 mL/min). Samples were exposed to a thermal cycle of heating from −60 to 120°C, then cooling from 120 to −60°C and a second heating from −60 to 250°C. The heating rate for all cycles was 10°C/min. The melting temperature (T_m) and the crystallization temperature (T_c) are reported for the PCL film and the bilayer films, PCL-eGR$_{DCM}$ and PCL-eGR$_{CF}$.

Thermogravimetric analysis (TGA) was performed in a TGA PT1000 from Linseis (Selb, Germany). Samples were heated under the TGA dynamic mode from 30 to 700°C at a heating rate of 10°C/min under a nitrogen atmosphere (flow rate 30 mL/min). The onset degradation temperatures ($T_{5\%}$) were determined at 5% of mass loss, while temperatures of the maximum decomposition rate (T_{max}) were obtained from the peak of the first derivative of the TGA curve (DTG). Both temperatures are reported for each film.

Mechanical analyses

Mechanical properties were measure through a tensile test, which was conducted in the PCL film and in the bilayer PCL-eGR films of an initial length of 50 mm and a width of 10 mm, according to standard tests methods ISO 527 part 3. The analyses were done at room temperature in an Elib 30 SAE Ibertest (Madrid, Spain) with a 100 N load cell, at a crosshead speed of 500 mm/min. Five specimens of each film were used. The mean value and the standard deviation of Young's modulus, tensile strength, and elongation at break are reported. The mechanical results were statistically analyzed at 95% confidence, as stated above.

3 | RESULTS

3.1 | Optimization of the processing of GR electrospraying process

It is known that to prepare appropriate solvent-based electrospray solutions, materials should be homogeneously dissolved in a proper solvent. An effective solvent should present a similar solubility parameter (δ) to that of the dissolved substance. The calculated solubility parameter for GR is 16.0 MPa$^{1/2}$, while CF and DCM have solubility parameters of 19 MPa$^{1/2}$ [9] and 20.2 MPa$^{1/2}$,[9], respectively. Since differences between GR and both solvents are moderately low, good miscibility and, thus, solubility in both solvents used should be expected.

The GR electrospray solutions were processed into electrosprayed microspheres varying the electrospraying processing conditions as are reported in Table 1. Meanwhile, the SEM images of each experiment are reported in Figure 1 for eGR$_{DCM,}$ and in Figure 2 for eGR$_{CF}$. The FESEM images of the GR microspheres show that the variations in solution flow rate and voltage applied produce differences in the morphology of GR microparticles.

Figure 1 shows that, when DCM is used as a solvent, a flow rate of 0.5 μL/min produces microspheres at all the assayed voltages. Flow rates of 1 and 5 μL/min produce microspheres at voltages of 10 and 15 kV. Meanwhile, a flow rate of 10 μL/min, produces defects such as beads at any voltage, which suggests that this flow does not allow the proper evaporation of the solvent. Therefore, it is not feasible to carry out an effective electrospraying process with GR in DCM operating at 10 μL/min. Moreover, it is observed that for flow rates of 1, 5 and 10 μL/min, an increase in the voltage produces an increase in the production of defects such as beads (Figure 1(D)–(L)). This is explained because the increment in the electrical forces destabilized the jet.[20,28,29] In brief, the experiments that allow the production of GR microspheres using DCM as solvent are a, b, c, d, e, g, and h.

The histograms presented in Figure 1, let to determine that the distribution is broad in experiments a, b, c, and e and narrow in experiments d, g, and h. Therefore, from the obtained results it can be concluded that the best processing conditions to obtain microspheres of GR$_{DCM}$ with uniform size are 1 μL/min and 10 kV corresponding to experiment d, which have the narrowest microspheres distribution. At the selected conditions microspheres with a mean diameter of 5 μm are obtained. Moreover, the smallest microsphere mean diameter was 4 μm, obtained with a flow of 0.5 μL/min and a potential of 20 kV. In Table 1 it is seen that for a flow rate of 0.5 μL/min (experiments b and c) a statistically significant ($p < 0.05$) microsphere diameter diminution is observed with the voltage increment, which is in good agreement with the literature.[11] For flow rates of 1 and 5 μL/min (experiments d, e, and g, h, respectively) the diameter size presents no statistical differences ($p > 0.05$) for the same flow. The density and the mean diameter of the microspheres are shown in Table 1.

Figure 2 presents the FESEM images of GR microspheres obtained from electrospraying using CF as solvent. For any flow rate, a mixture between microfibers and microspheres is obtained at voltages of 15 and 20 kV, except in experiment h. A similar effect has been observed in the work of Bock et al., who work with PCL dissolved in CF in concentrations of 5, 7.5, 9, and 10% w/v and obtain microspheres contaminated with nanofibers of the same material when using high concentrations of polymer and low solution flow rates.[8] This could indicate that the concentration of 45 w/v of GR solution with CF is too high for an electrospraying process at the higher voltages assayed here of 15 and 20 kV for all flow rates assayed (except for 5 μL/min and 15 kV).[8] Therefore, when using CF as a solvent, the experiments that allowed to obtain microspheres are a, d, g, h, and j.

Regarding the size distribution, it is seen that in experiments a, d, and g it is narrow and in experiments h and j there is a broader size distribution. Therefore, the best conditions to obtain microspheres of

TABLE 1 Flow rate and potential conditions used for the experiments, density and means size of the microspheres obtained with different solvents

			DCM		CF	
Experiment	Flow rate (μL/min)	Voltage (kV)	Microspheres density (microspheres/μm^2) × 1000	Microspheres diameter (μm)	Microspheres density (microspheres/μm^2) × 100	Microspheres diameter (μm)
a	0.5	10	8.73 ± 0.37^a	6 ± 2^a	2.52 ± 0.14^a	4 ± 1^a
b	0.5	15	4.31 ± 0.44^b	8 ± 2^b	*	*
c	0.5	20	4.95 ± 0.38^b	4 ± 2^c	*	*
d	1	10	7.42 ± 0.36^{a,b}	5 ± 2^c	40.41 ± 0.34^b	3 ± 1^a
e	1	15	34.8 ± 2.91^c	4 ± 1^c	*	*
f	1	20	*	*	*	*
g	5	10	9.17 ± 0.14^a	7 ± 2^b	1.01 ± 0.20^c	5 ± 1^b
h	5	15	7.28 ± 0.25^{a,b}	7 ± 1^b	1.07 ± 0.20^c	5 ± 1^b
i	5	20	*	*		
j	10	10	*	*	0.15 ± 0.06^d	6 ± 1^b
k	10	15	*	*	*	*
l	10	20	*	*	*	*

Note: Different letters (a–c) show statistically significant differences between formulations ($p < 0.05$).
*No microspheres produced.

GR_{CF} with uniform size were 5 μL/min and 10 kV, corresponding to experiment g, which showed the narrowest particle size distribution. At the selected condition microspheres with a mean diameter of 5 μm are obtained. Table 1 shows the density and the mean diameter of the microspheres obtained by electrospraying of GR solutions with CF. It is seen that, at a voltage of 10 kV, an increase in the flow rate (experiments d and g) produces a significant increase in the diameter of the microspheres. These results are in accordance with those obtained by Khan et al., who concludes that the contact time of the solution in the needle is inversely proportional to the size of the sphere obtained.[11] For a flow rate of 5 μL/min, an increase in the voltage (experiments g and h) does not produce significant changes in the diameter size of the microsphere ($p > 0.05$). With CF, the smallest mean diameter was 3 μm, and it was obtained with a flow of 1 μL/min and a potential of 10 kV.

The obtained results allow inferring that uniform size GR microspheres can be produced using either DCM or CF as a solvent and that the size distribution can be adjusted changing either the flow rate of the solution or the voltage applied. In both systems, the electrospraying parameters selected produced microspheres with a statistically equal mean size of 5 μm.

3.2 | Bilayer film characterization

3.2.1 | Visual appearance, colorimetric and UV–Vis spectroscopic analyses

The visual appearances of neat PCL and PCL-eGR bilayer films are shown in Figure 3. While PCL film is transparent allowing seen through the film (Figure 3(A)), the presence of GR reduced the transparency in bilayer PCL-eGR films and also showing somewhat yellow tonality (PCL-eGR_{DCM} in Figure 3(B) and PCL-eGR_{CF} in Figure 3(C)), confirming the successful deposition of GR onto the PCL film as GR is yellow (Figure 3(D)). These findings were corroborated by colorimetric measurements and UV–vis analysis.

Regarding the color parameters (Table 2) it is seen that PCL and both bilayers present a high value of L* (>79), which is a characteristic of bright whitish colored objects, meanwhile GR have a lower value of L* (52), because the material is darker, therefore, it has greater absorbance and less total reflectance for what it has lower lightness.[30] The a* coordinate value is near zero in all the materials, which suggest that neither red nor green colorations are dominant.[27] The b* coordinate is negative in PCL, which reveals a faint blue hue in the material. On the other hand, PCL-eGR_{DCM} and PCL-eGR_{CF}, have positive values of b* showing yellow coloration in the samples.[27] Yellow hue value in neat GR is evident, and accordingly presents the highest b* value, which suggests that the natural color of GR influences the coloration of the electrosprayed layer,[19] in agreement with the visual appearance of the films. Regarding the yellowness index (YI), its values are in accordance with the b* coordinate, being GR the sample with the highest YI as expected, followed by PCL-eGR_{CF}, then by PCL-eGR_{DCM}, both with positive YI values, and finally PCL with the lowest and negative YI value. It is seen that The YI index of PCL-GR bilayers is among the values of the components, neat GR, and PCL. Nevertheless, it should be highlighted that the color of the bilayers differs drastically from the color of neat GR, which is due to GR microspheres. Neat GR occurs in the form of angular, translucent masses of various sizes,[31] while the microspheres are smaller and have a different geometrical shape than GR. The color depends on the optical reflection properties of the object, therefore, the highlights, shadows, and shading influence the perception of the color.[32] In addition, as observed in Table 2 the

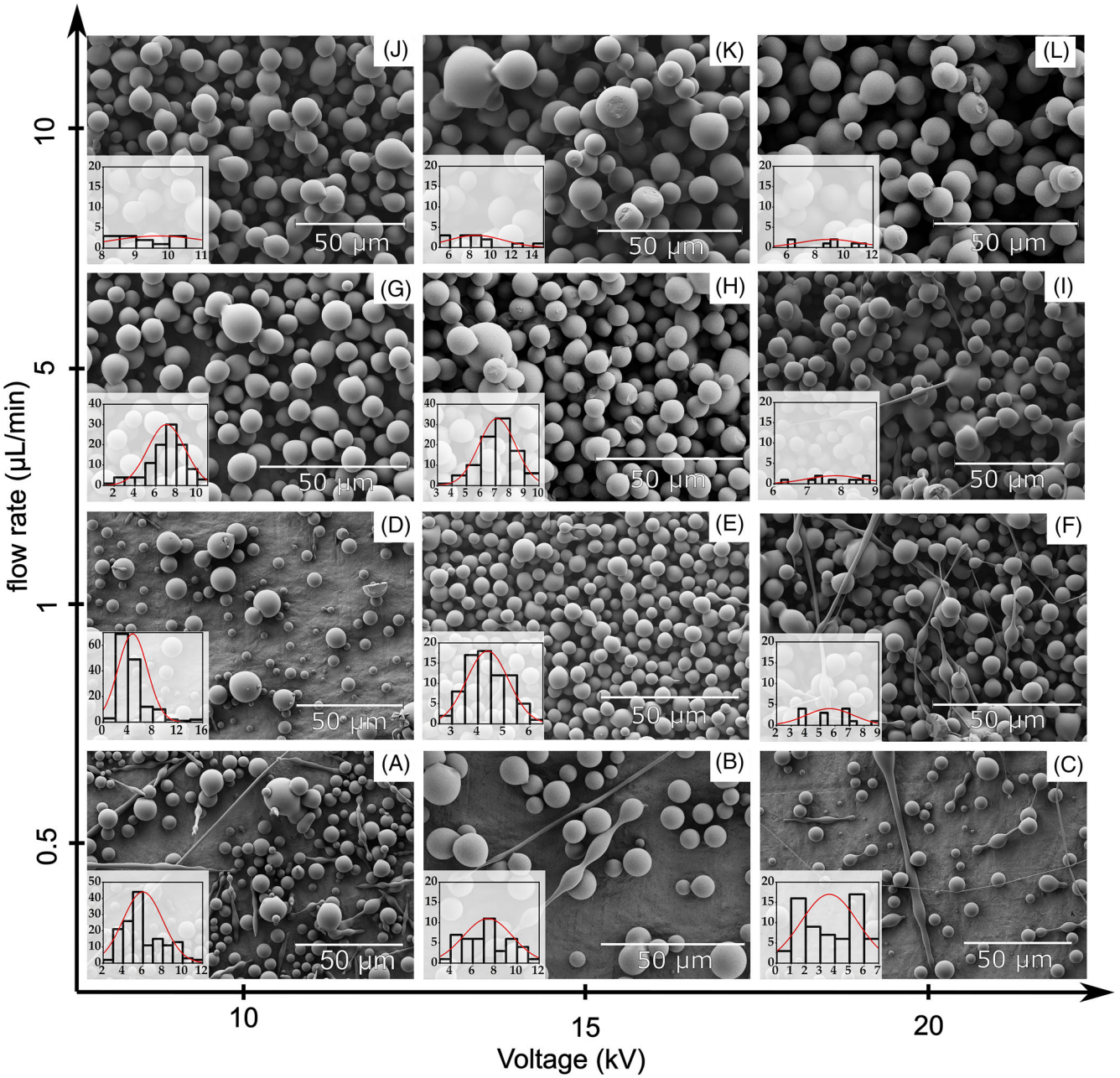

FIGURE 1 Micrographs of gum rosin microspheres produced by electrospraying using DCM as solvent: flow rate as a function of voltage. Flow rate of 0.5 μL/min and a potential of (A) 10 kV, (B) 15 kV, (C) 20 kV. Flow rate of 1 μL/min and potential (D) 10 kV, (E) 15 kV, and (F) 20 kV. Flow rate of 5 μL/min and potential (G) 10 kV, (H) 15 kV, (I) 20 kV, and flow rate of 10 μL/min and potential (J) 10 kV, (K) 15 kV, and (L) 20 KV. Size distribution is shown as a histogram

color parameters are statistically different in both bilayers, which is due to the higher amount of GR deposited over PCL film during the 4 h electrospraying process in the case of PCL-eGR$_{CF}$, since electrospraying flow rate is higher (5 μL/min) than that of GRD$_{DCM}$ (1 μL/min). Moreover, these differences could be also attributed to the different particle shape obtained in the electrospraying process.[32] The visual appearance of PCL film, PCL-GR bilayer films and GR along with their yellow index is presented in Figure 3.

UV–Vis spectra of PCL, PCL-eGR$_{DCM,}$ and PCL-eGR$_{CF}$ (Figure S1). PCL spectrum presents an increment of the absorption intensity in the range of 240–340 nm, related to carbonyl groups (C═O).[33] In addition, the presence of PCL characteristic absorption band is seen at 280 nm.[34] No absorption peaks are seen at longer wavelength >280 nm as reported in the literature.[34] The UV- Vis spectra of the bilayer films present a significant increase of the absorbance intensity in the carbonyl groups region and the presence of two sharp bands, associated with the absorption of different types of carbonyl groups.[33] The changes in respect to the neat PCL film spectrum are attributed to the presence of GR. According to the literature, GR displays significant absorption in UV spectroscopy

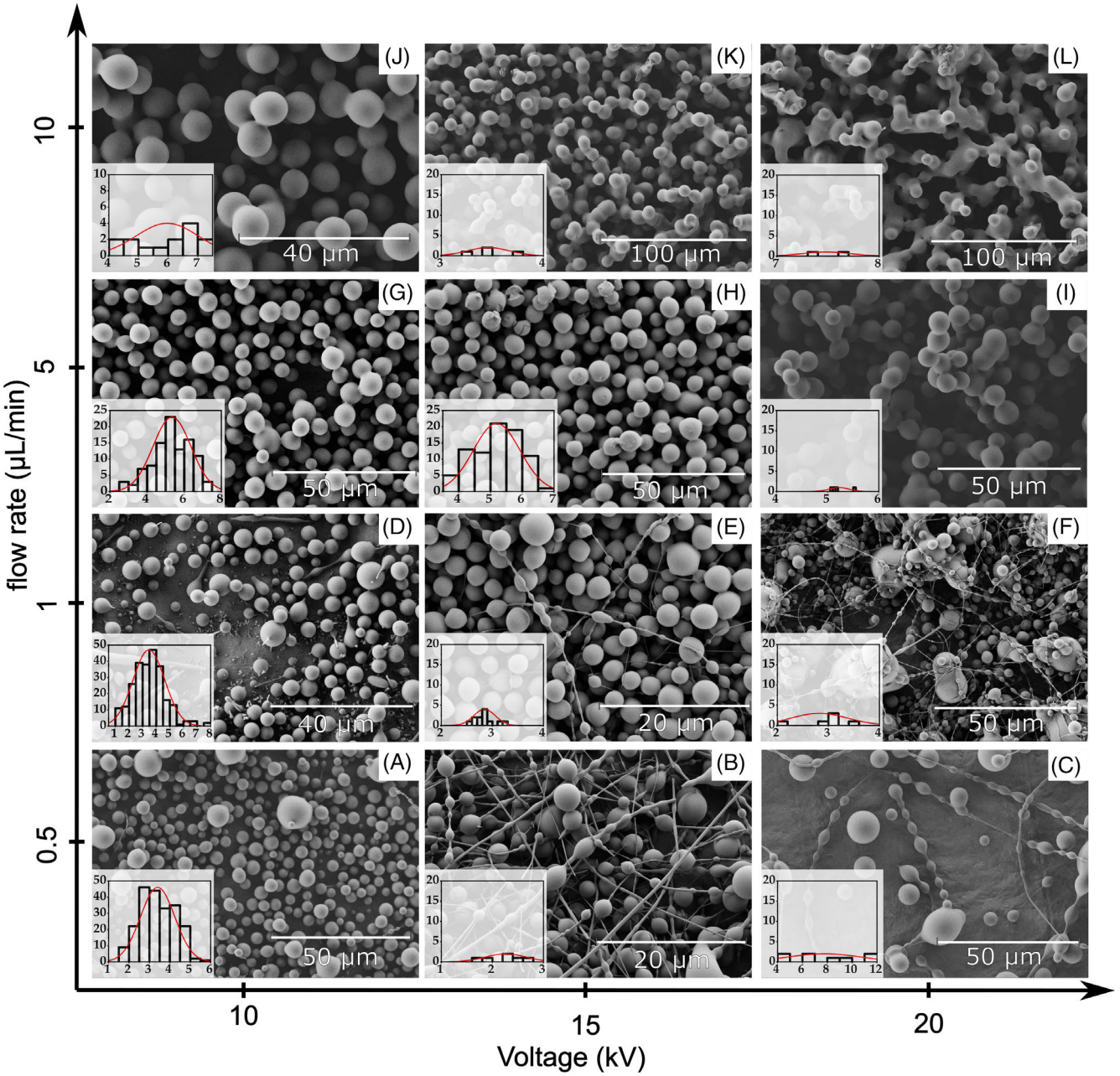

FIGURE 2 Micrographs of gum rosin microspheres produced by electrospraying using CF as solvent: flow rate as a function of voltage. Flow rates of 0.5 µL/min and potential of (A) 10 kV, (B) 15 kV, (C) 20 kV. Flow rate of 1 µL/min and potential (D) 10 kV, (E) 15 kV, and (F) 20 kV. Flow rate of 5 µL/min and potential (G) 10 kV, (H) 15 kV, (I) 20 kV, and flow rate of 10 µL/min and potential (J) 10 kV, (K) 15 kV, and (L) 20 KV. Size distribution is shown as a histogram

because of the conjugated group.[35] Moreover, two bands are observed in the PCL-eGR$_{DCM}$ and PCL-eGR$_{CF}$ spectra located at 205 and 258 nm, which are typical of GR.[36]

In Figure S1 it is possible to observe that while PCL showed high transmission in the visible region of the spectra, the microspheres layer reduced the transmission in bilayer systems. Both bilayers present a complete radiation-blocking in the UVB region (280–320 nm) and the UVA region until 345 nm, where the transmittance begins to increase. The blocking effect in what remains of the UVA zone is high, with a transmittance of 15% at 400 nm. Therefore, the GR microspheres provide a protective effect in the UV region of the spectra. Similarly, it has been observed that GR acts as a light-absorbing agent and prevents the transmission of light through PLA-GR-based films.[17] PCL-eGR$_{DCM}$ bilayer formulation has somewhat lower transmittance than PCL-eGR$_{CF}$ in the visible region of the spectra, which could be attributed to the morphology of the microspheres with the presence of beads defects.

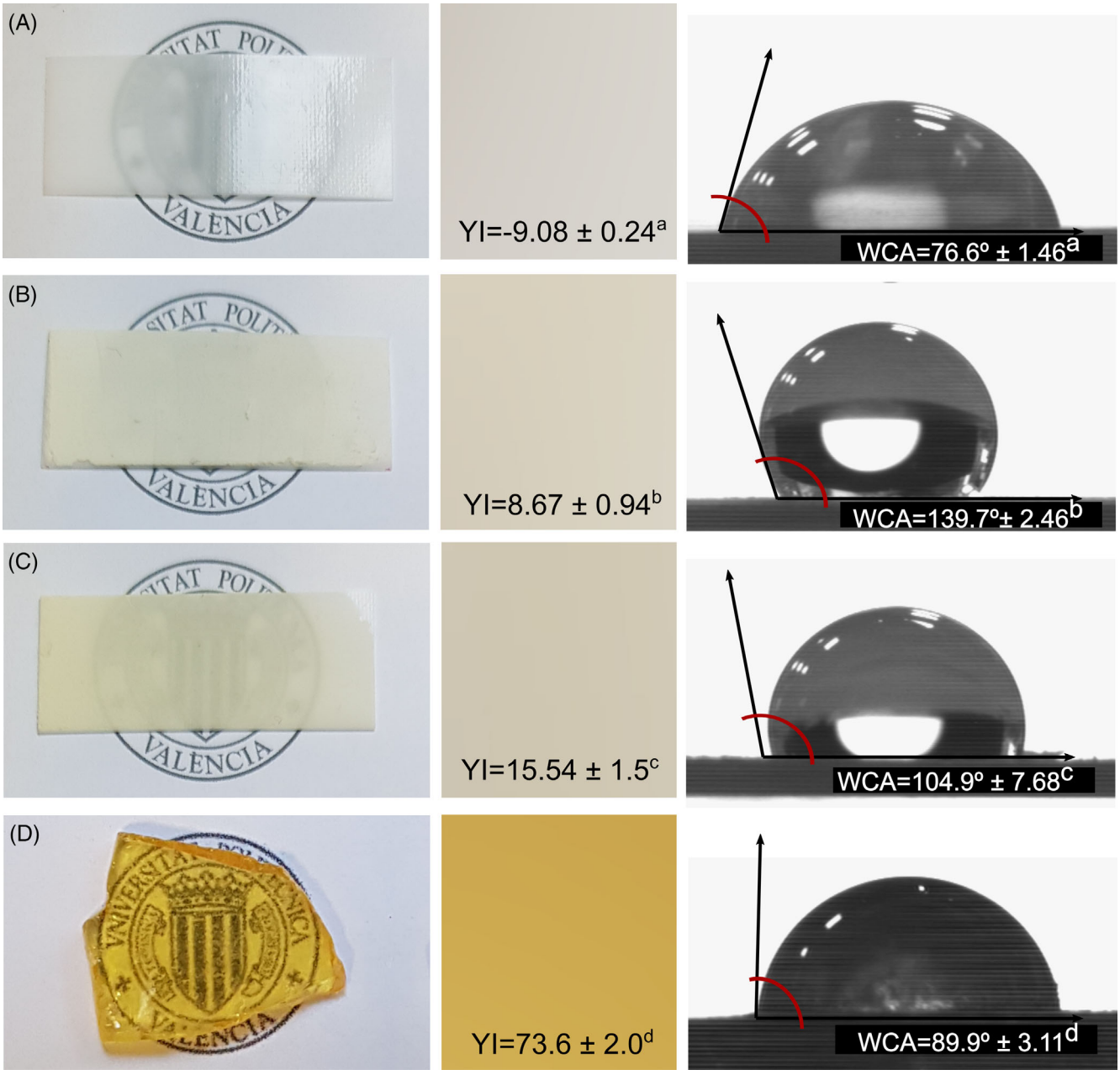

FIGURE 3 Visual appearance, yellowness index, and water contact angle of (A) PCL, (B) PCL-eGRDCM, (C) PCLeGRCF films, and (D) neat GR. Different letters (a–d) show statistically significant differences between formulations ($p < 0.05$)

TABLE 2 Color parameters for the CIEL*a*b* space of neat PCL film, GR, and the bilayers PCL-eGR$_{DCM}$ and PCL-eGR$_{CF}$

Code	L*	a*	b*	YI	ΔE
PCL	79.66 ± 0.90^{a}	−0.89 ± 0.06^{a}	−3.39 ± 0.10^{a}	−9.08 ± 0.24^{a}	0.77 ± 0.40
PCL-eGR$_{DCM}$	89.09 ± 0.67^{b}	−1.92 ± 0.15^{b}	4.87 ± 0.50^{b}	8.67 ± 0.94^{b}	12.58 ± 0.58
PCL-eGR$_{CF}$	83.94 ± 1.51^{c}	−2.86 ± 0.36^{c}	7.01 ± 1.93^{c}	15.54 ± 1.50^{c}	11.44 ± 2.32
Neat GR	52.8 ± 0.9^{d}	−0.3 ± 0.1^{d}	26.6 ± 0.8^{d}	73.6 ± 2.0^{d}	49.22 ± 18.8

Note: Different letters (a–d) show statistically significant differences between formulations ($p < 0.05$).

3.2.2 | Water contact angle

PCL and GR present a hydrophobic character as stated in literature.[19,37] Nonetheless, the incorporation of GR microspheres layer over PCL film significantly increases the WCA in bilayer formulations, in values higher than GR in its neat form (see Figure 3). The surface wettability is highly dependent on the surface topographical and chemical properties. On the one hand, the shape of the microspheres can increase the contact

surface changing the topography. On the other hand, the hydroxyl groups of GR can be interacting with GR through hydrogen bond interactions that are favoring the interaction among both layers. Therefore, the inherent hydrophobicity of GR will be enhanced in the bilayer with respect to neat GR and PCL film. In addition, the WCA in PCL-eGR$_{DCM}$ is higher than in PCL-eGR$_{CF}$ reaching values often defined as ultra-hydrophobic surfaces (WCA > 120°),[38] even when having a lower amount of GR. This behavior is because the hydroxyl groups of GR are not available to interact with water and the shape of the deposited particles varies in a wide-ranging shape when DCM is used as a solvent as seen in the SEM micrographs (Figure 4) and thus, the topographic of the surface is highly influenced. Consequently, the contact surface in PCL-eGR$_{DCM}$ would be higher than PCL-eGR$_{CF}$,

3.2.3 | Optical and scanning electron microscopy

Figure 4 shows the surface and cross-section of neat PCL and PCL-eGR bilayers systems. The neat PCL showed a non-porous and smooth microstructural surface typical of PCL based formulations.

Even when the electrospraying process has been optimized, the obtained particles did not form only microspheres, but a mixture of microspheres and beads was observed when DCM is used as a solvent.

This could be explained because the use of natural materials is difficult in electrohydrodynamic processes since the properties of the raw materials are highly variable.[29] Furthermore, according to Bhardwaj and Kundu, natural materials are mostly polyelectrolytic, so that the ions in their structure contribute a greater charge to the solution.[28] Hence, the ability to form microstructures will also depend on the composition or acid content of the GR used, which gives the electrolytic character to the material.[39] The formation of beads during electrohydrodynamic processes has been also related to the low similarity between components of the polymeric solution.[25] Therefore, considering that CF was able to produce microspheres with fewer beads defects, it can also be ascribed with the closer solubility parameter between GR and CF, than those between GR and DCM.

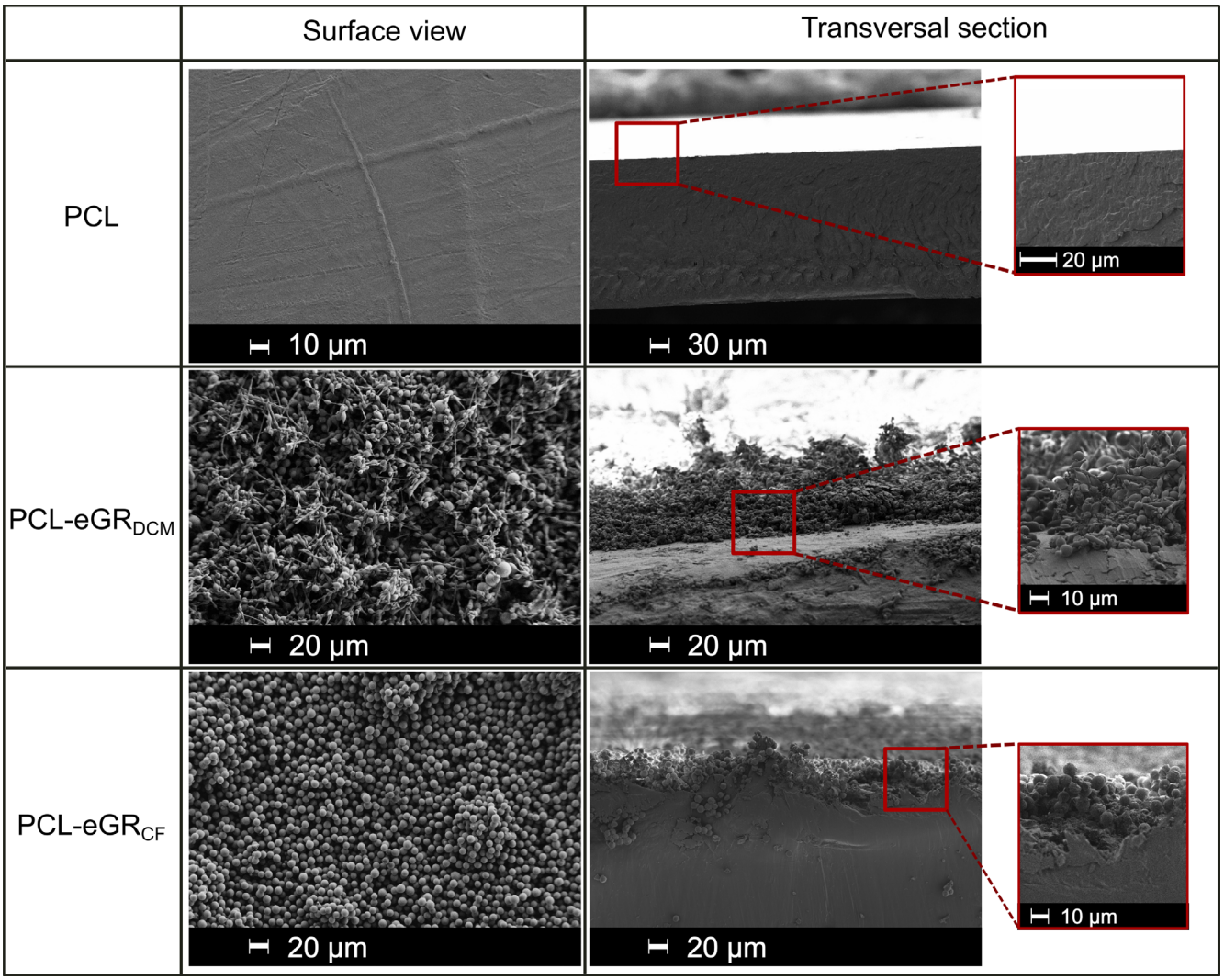

FIGURE 4 Scanning electron microscope (SEM) observations of PCL and the bilayer films PCL-eGRDCM and PCL-eGRCF of surface and transversal section with the expanded area

TABLE 3 DSC and TGA results of neat PCL film, GR, and electrosprayed bilayer PCL-eGR$_{DCM}$ and PCL-eGR$_{CF}$

Code	T_c (°C)	ΔH_c (J/g)	T_m (°C)	ΔH_m (J/g)	$T_{5\%}$ (°C)	T_{max} (°C)
PCL	27.85	71.13	57.75	−62.06	330.56	412.06
PCL-eGR$_{DCM}$	25.51	70.13	57.01	−60.31	337.47	413.47
PCL-eGR$_{CF}$	28.86	71.68	56.59	−63.45	334.68	414.68
GR	52.81	3.87	50.02	−6.30	228.15	313.25

3.2.4 | Thermal analyses

The thermal parameters obtained from DSC and TGA analyses are summarized in Table 3. According to literature PCL films presents a melting temperature around 60°C, and the melting enthalpy approximately 60 J/g,[19,40] which is in accordance with the obtained values. The $T_{5\%}$ and T_{max} values measured in the TGA also agree with the literature.[19] As seen in Table 3, the thermal parameter of GR are considerably higher than those of PCL and the obtained for the bilayer systems, therefore, it can be inferred that the GR microspheres layer did not affect significantly the PCL thermal stability mostly because the mass proportion of GR is to low.[41] It should be highlighted that the obtained formulations are thermally stable in the range of room temperature to higher than 300°C, which is a considerably higher temperature than that of the intended use (i.e., mulch film, food packaging, etc.).

3.2.5 | Mechanical analyses

Neat PCL film presents Young's modulus of 109 ± 7 MPa, a tensile strength of 17 ± 1 MPa, and elongation at break of 1173% ± 50%. No statistical differences can be found in Young's modulus and elongation at break of PCL and the PCL-eGR bilayer systems. This suggests that the deposited layer is too thin to produce a significant change in the tensile performance of the PCL film. However, a significant reduction in the tensile strength is observed in the bilayers with respect to neat PCL. Tensile strength for PCL-eGR$_{DCM}$ is 13 ± 1 MPa while tensile strength for PCL-eGR$_{CF}$ is 14 ± 1 MPa. This reduction is approximately 20% and both bilayers have no statistical differences in tensile strength. This reduction in the tensile strength is probably due to the composite structure and the lower tensile strength of GR, which affect the overall performance of the bilayer system. In fact, it has been observed that GR reduces the tensile strength of PCL in PCL/GR-based blends.[19] Although the tensile strength values suggest the risk of film cracking, no sign of cracking in bilayer films was observed, which may partly be attributed to the superior viscoelastic performance of PCL. In fact, the high flexibility of PCL was not affected by the GR microspheres, and it is probably that the very thin layer of GR broke before the PCL layer in the bilayer structure during the tensile test measurements. However, this behavior is frequently undetectable from the stress to strain curve (not shown) when very thin layers are used.[26]

4 | CONCLUSIONS

The processing conditions to obtain GR microspheres by electrospraying technique using DCM and CF as solvents were successfully optimized and both PCL-eGR$_{DCM}$ and PCL-eGR$_{CF}$ bilayer films were successfully obtained. It was determined that the best conditions to obtain microspheres with a uniform size of 5 μm are 1 μL/min and 10 kV when DCM is used as a solvent, and 5 μL/min and 10 kV when CF is used as a solvent. Besides it was seen that GR$_{CF}$ solution mainly leads to electrospray microspheres without defects and GR$_{DCM}$ solution produced eGR$_{DCM}$ microspheres whit some beads defects. The lower formation of beads in eGR$_{CF}$ microspheres with respect to eGR$_{DCM}$ microspheres has been ascribed to the smaller differences between the solubility parameters of GR with CF compared with that of the DCM.

The GR microspheres layered onto PCL film produced significant changes in the surface color and an increase in the surface hydrophobicity with respect to both, neat GR and neat PCL, as the water contact angle considerably increased. This behavior has been ascribed to the positive chemical interaction of GR layer with PCL layer as well as to the size of the microspheres, which are able to increase the contact surface of GR and the roughness in the material surface. In fact, PCL-eGR$_{DCM}$ showed considerably improved surface hydrophobicity reaching values of ultrahydrophobic surface.

The thermal and mechanical performance of PCL film is not affected by the deposition of GR microspheres. In addition, PCL-eGR$_{DCM}$ and PCL-eGR$_{CF}$ presented a complete radiation-blocking in the UVB region and a high blockage in the UVA zone, with a small reduction in the transparency of the neat PCL film.

In summary, we have developed a facile and scalable strategy to develop translucent PCL-eGR bilayer systems with UV blocking effect without compromising the mechanical and thermal performance of PCL, with tunable hydrophobicity depending on the solvent use, which could be of interest for the food packaging industry. Furthermore, it is worth noting that the dimensions of the eGR microsphere present allotropic advantages with respect to the macroscopic material. In fact, although further studies are required, because of eGR microsphere large surface area, they have great potential to carry drugs, nanoparticles, and active substance, which makes these microspheres interest in the biomedical and active materials field for sustainable agricultural or packaging applications.

ACKNOWLEDGEMENTS

C.P. thanks Santiago Grisolía fellowship (GRISOLIAP/2019/113) from Generalitat Valenciana. M.P.A. thanks Secretaría de Educación Superior, Ciencia, Tecnología e Innovación (SENESCYT) and Escuela Politécnica Nacional (EPN).

CONFLICT OF INTEREST

The authors declare no conflict of interest.

DATA AVAILABILITY STATEMENT

The data presented in this study are available on request from the corresponding author.

ORCID

Cristina Pavon https://orcid.org/0000-0003-2902-0059
Miguel Aldas https://orcid.org/0000-0003-3491-6618
Harrison De La Rosa-Ramírez https://orcid.org/0000-0002-2913-7938
María Dolores Samper https://orcid.org/0000-0002-5102-8412
Marina Patricia Arrieta https://orcid.org/0000-0003-1816-011X
Juan López-Martínez https://orcid.org/0000-0001-6904-2282

REFERENCES

1. Bai F, Yang X, Li R, Huang B, Huang W. Monodisperse hydrophilic polymer microspheres having carboxylic acid groups prepared by distillation precipitation polymerization. *Polymer*. 2006;47(16):5775-5784. https://doi.org/10.1016/j.polymer.2006.06.014.
2. Li S, Yang X, Huang W. Synthesis of monodisperse polymer microspheres with mercapto groups and their application as a stabilizer for gold metallic colloid. *Macromol Chem Phys*. 2005;206(19):1967-1972. https://doi.org/10.1002/macp.200500216.
3. Wang Z, Lei FH, Li W, et al. Preparation of rosin-based polymer microspheres as a stationary phase in high-performance liquid chromatography to separate polycyclic aromatic hydrocarbons and alkaloids. *E-Polymers*. 2019;19(1):290-296. https://doi.org/10.1515/epoly-2019-0029.
4. Hossain KMZ, Patel U, Ahmed I. Development of microspheres for biomedical applications: a review. *Prog Biomater*. 2015;4(1):1-19. https://doi.org/10.1007/s40204-014-0033-8.
5. More RK, Sonawane DS, Patil MP, Kshirsagar SJ. An overview: use of polymer microspheres in controlled drug delivery. *Res J Pharm Dos Forms Technol*. 2018;10(3):193. https://doi.org/10.5958/0975-4377.2018.00030.7.
6. Anu Bhushani J, Anandharamakrishnan C. Electrospinning and electrospraying techniques: potential food based applications. *Trends Food Sci Technol*. 2014;38(1):21-33. https://doi.org/10.1016/j.tifs.2014.03.004.
7. Jaworek A. Micro- and nanoparticle production by electrospraying. *Powder Technol*. 2007;176(1):18-35. https://doi.org/10.1016/j.powtec.2007.01.035.
8. Bock N, Woodruff MA, Hutmacher DW, Dargaville TR. Electrospraying, a reproducible method for production of polymeric microspheres for biomedical applications. *Polymers*. 2011;3(1):131-149. https://doi.org/10.3390/polym3010131.
9. Arrieta MP, García AD, López D, Fiori S, Peponi L. Antioxidant bilayers based on PHBV and plasticized electrospun PLA-PHB fibers encapsulating catechin. *Nanomaterials*. 2019;9(3):1-14. https://doi.org/10.3390/nano9030346.
10. Qian W, Li X-Y, Yu D-G, et al. Polymer-based nanoparticulate solid dispersions prepared by a modified electrospraying process. *J Biomed Sci Eng*. 2011;4(12):741-749. https://doi.org/10.4236/jbise.2011.412091.
11. Khan MKI, Nazir A, Maan AA. Electrospraying: a novel technique for efficient coating of foods. *Food Eng Rev*. 2017;9(2):112-119. https://doi.org/10.1007/s12393-016-9150-6.
12. Rodríguez-García A, Martín JA, López R, Mutke S, Pinillos F, Gil L. Influence of climate variables on resin yield and secretory structures in tapped *Pinus pinaster* Ait. in Central Spain. *Agric Meteorol*. 2015;202:83-93. https://doi.org/10.1016/j.agrformet.2014.11.023.
13. Kumar S, Gupta SK. Rosin: a naturally derived excipient in drug delivery systems. *Polim Med*. 2013;43(1):45-48. https://doi.org/10.1364/JOSAA.22.001380.
14. Wilbon PA, Chu F, Tang C. Progress in renewable polymers from natural terpenes, terpenoids, and rosin. *Macromol Rapid Commun*. 2013;34(1):8-37. https://doi.org/10.1002/marc.201200513.
15. Aldas M, Pavon C, López-Martínez J, Arrieta MP. Pine resin derivatives as sustainable additives to improve the mechanical and thermal properties of injected moulded thermoplastic starch. *Appl Sci*. 2020;10(7):2561. https://doi.org/10.3390/app10072561.
16. de la Rosa-Ramirez H, Aldas M, Ferri JM, Samper MD, Lopez-Martinez J. Modification of poly (lactic acid) through the incorporation of gum rosin and gum rosin derivative: mechanical performance and hydrophobicity. *J Appl Polym Sci*. 2020;137:49346. https://doi.org/10.1002/app.49346.
17. Narayanan M, Loganathan S, Babu R, et al. UV protective poly (lactic acid)/rosin films for sustainable packaging. *Int J Biol Macromol*. 2017;99:37-45. https://doi.org/10.1016/j.ijbiomac.2017.01.152.
18. Pratapwar A, Sakarkar D. Applications of rosin derivatives in the development of novel drug delivery system (NDDS): a contemporary view. *J Qual Assur Pharma Anal*. 2015;1(1):100-109.
19. Pavon C, Aldas M, López-Martínez J, Ferrándiz S. New materials for 3D-printing based on polycaprolactone with gum rosin and beeswax as additives. *Polymers*. 2020;12(2):334. https://doi.org/10.3390/polym12020334.
20. Arrieta MP, Leonés Gil A, Yusef M, Kenny JM, Peponi L. Electrospinning of PCL-based blends: processing optimization for their scalable production. *Materials*. 2020;13(17):3853. https://doi.org/10.3390/ma13173853.
21. Baek WI, Nirmala R, Barakat NAM, El-Newehy MH, Al-Deyab SS, Kim HY. Electrospun cross linked rosin fibers. *Appl Surf Sci*. 2011;258(4):1385-1389. https://doi.org/10.1016/j.apsusc.2011.09.082.
22. Nirmala R, Baek W, Navamathavan R, et al. Bactericidal efficacy of electrospun rosin/poly(ϵ-caprolactone) nanofibers. *Macromol Res*. 2014;22(2):139-145. https://doi.org/10.1007/s13233-014-2017-x.
23. Nirmala R, Woo-il B, Navamathavan R, Kim HY, Park S-J. Preparation and characterizations of rosin based thin films and fibers. *J Nanosci Nanotechnol*. 2015;15(6):4653-4659. https://doi.org/10.1166/jnn.2015.9596.
24. Figueroa-Lopez KJ, Cabedo L, Lagaron JM, Torres-Giner S. Development of electrospun poly(3-hydroxybutyrate-co-3-hydroxyvalerate) monolayers containing eugenol and their application in multilayer antimicrobial food packaging. *Front Nutr*. 2020;7:140. https://doi.org/10.3389/fnut.2020.00140.
25. Arrieta MP, López de Dicastillo C, Garrido L, Roa K, Galotto MJ. Electrospun PVA fibers loaded with antioxidant fillers extracted from Durvillaea Antarctica algae and their effect on plasticized PLA bionanocomposites. *Eur Polym J*. 2018;103:145-157. https://doi.org/10.1016/j.eurpolymj.2018.04.012.
26. Arrieta MP, Garrido L, Faba S, Guarda A, Galotto MJ, de Dicastillo CL. *Cucumis metuliferus* fruit extract loaded acetate cellulose coatings for antioxidant active packaging. *Polymers*. 2020;12(6):1248. https://doi.org/10.3390/POLYM12061248.
27. Luo MR. CIELAB. *Encyclopedia of Color Science and Technology*. Berlin: Springer; 2015:1-7.
28. Bhardwaj N, Kundu SC. Electrospinning: a fascinating fiber fabrication technique. *Biotechnol Adv*. 2010;28(3):325-347. https://doi.org/10.1016/j.biotechadv.2010.01.004.
29. Liu G, Gu Z, Hong Y, Cheng L, Li C. Electrospun starch nanofibers: recent advances, challenges, and strategies for potential pharmaceutical applications. *J Control Release*. 2017;252:95-107. https://doi.org/10.1016/j.jconrel.2017.03.016.
30. Hernández B, Sáenz C, Alberdi C, Diñeiro JM. CIELAB color coordinates versus relative proportions of myoglobin redox forms in the

description of fresh meat appearance. *J Food Sci Technol*. 2016;53 (12):4159-4167. https://doi.org/10.1007/S13197-016-2394-6.

31. Yadav BK, Gidwani B, Vyas A. Rosin: recent advances and potential applications in novel drug delivery system. *J Bioact Compat Polym*. 2016;31(2):111-126. https://doi.org/10.1177/0883911515601867.
32. Klinker G, Shafer SA, Kanade T. The measurement of highlights in color images. *Int J*. 1988;32:7-32.
33. De Campos A, Martins Franchetti SM. Biotreatment effects in films and blends of PVC/PCL previously treated with heat. *Brazilian Arch Biol Technol*. 2005;48(2):235-243. https://doi.org/10.1590/s1516-89132005000200010.
34. Abdelrazek EM, Hezma AM, El-khodary A, Elzayat AM. Spectroscopic studies and thermal properties of PCL/PMMA biopolymer blend. *Egypt J Basic Appl Sci*. 2016;3(1):10-15. https://doi.org/10.1016/j.ejbas.2015.06.001.
35. Li Y, Liu X, Zhang Q, et al. Characteristics and kinetics of rosin pentaerythritol ester via oxidation process under ultraviolet irradiation. *Molecules*. 2018;23(11):2816. https://doi.org/10.3390/molecules23112816.
36. Liu JL, Liu XM, Li WG, Ma L, Shen F. Kinetics of gum rosin oxidation under 365 nm ultraviolet irradiation. *Monatsh Chem*. 2014;145(1): 209-212. https://doi.org/10.1007/s00706-013-1014-7.
37. Guarino V, Gentile G, Sorrentino L, Ambrosio L. *Polycaprolactone: Synthesis, Properties, and Applications*. Hoboken, NJ: John Wiley & Sons, Inc.; 2017.
38. De Francisco R, Tiemblo P, Hoyos M, et al. Multipurpose ultra and superhydrophobic surfaces based on oligodimethylsiloxane-modified nanosilica. *ACS Appl Mater Interfaces*. 2014;6(21):18998-19010. https://doi.org/10.1021/am504886y.
39. Karlberg AT. Colophony. In: *Handbook of Occupational Dermatology*. Springer, Berlin, Heidelberg. 2000:506-516. https://doi.org/10.1007/978-3-662-07677-4_64.
40. Borghesi DC, Molina MF, Guerra MA, Campos MGN. Biodegradation study of a novel poly-caprolactone-coffee husk composite film. *Mater Res*. 2016; 19(4):752-758. https://doi.org/10.1590/1980-5373-MR-2015-0586.
41. Yazovkin S. Thermogravimetric analysis. In: *Characterization of Materials*. Hoboken, NJ: John Wiley & Sons, Inc. 2012. https://doi.org/10.1002/0471266965.com029.pub2.

SUPPORTING INFORMATION

Additional supporting information may be found online in the Supporting Information section at the end of this article.

How to cite this article: Pavon C, Aldas M, De La Rosa-Ramírez H, Samper MD, Arrieta MP, López-Martínez J. Bilayer films of poly(ε-caprolactone) electrosprayed with gum rosin microspheres: Processing and characterization. *Polym Adv Technol*. 2021;32(9):3770–3781. https://doi.org/10.1002/pat.5397